Optimum Window: Source to Receiver

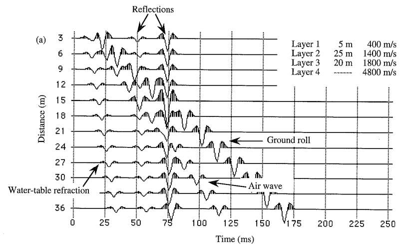

Figure 4-24 An illustration of the importance of source-receiver distance in reflection surveying. (a) Typical reflection record showing positions of low-velocity waves (ground roll and air wave), refraction from the water table, and reflections from two interfaces. (b) An increased source-geophone distance moves low-velocity waves toward greater time at a rate faster than reflections which become easier to discern. Position of optimum window indicated. (c) Increased bedrock depth moves the bedrock reflector toward increased time and changes the position of the optimum window for the bedrock reflection.

Optimum Window: Source Receiver Distance

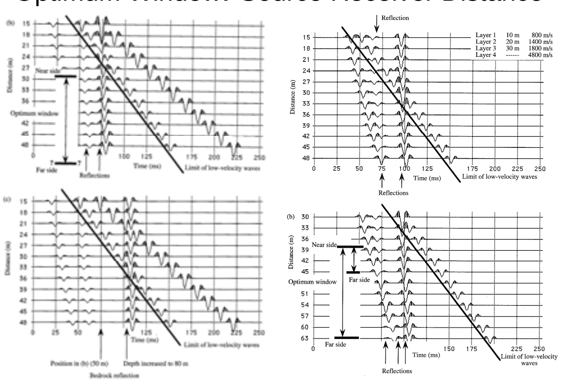

Optimum Window: Field Records

30 m offset

60 m offset
Different Site

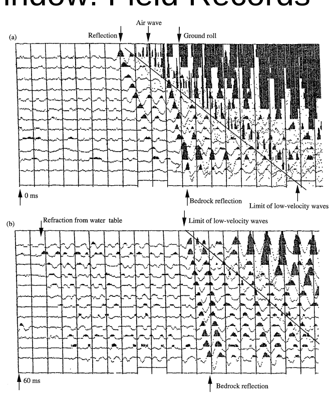

Multiples

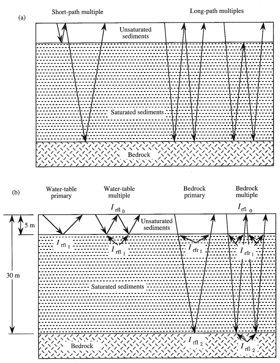

Multiples

TABLE 4.9 Relative Energy Comparisons Among Primary Reflections and Multiples

	Water-table Primary	Water-table Multiple	Bedrock Primary	Bedrock Multiple
Energy partitioning	1.000	0.359	0.353	0.045
Plus absorption	1.000	0.323	0.189	0.013
Plus spherical spreading	1.000	0.314	0.160	0.009

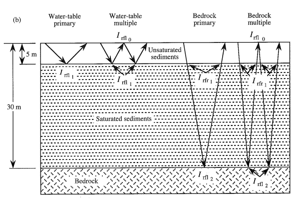

Multiples: Twice the Time Less NMO

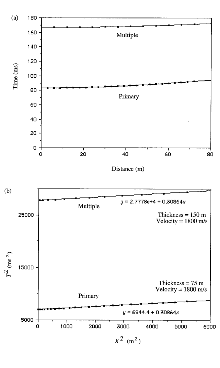

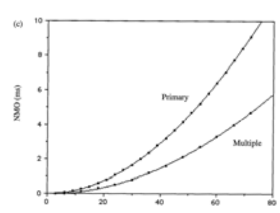

Diffractions

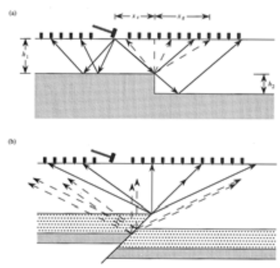

For diffraction travel-time

$$t_d = \frac{(x_d^2 + h_1^2)^{1/2}}{V_1} \quad (4\text{-}58)$$

Similarly, for travel-time from source to edge

$$t_s = \frac{(x_s^2 + h_1^2)^{1/2}}{V_1} \quad (4\text{-}59)$$

and, finally,

$$t_t = \frac{(x_s^2 + h_1^2)^{1/2}}{V_1} + \frac{(x_d^2 + h_1^2)^{1/2}}{V_1} \quad (4\text{-}60)$$

Diffractions

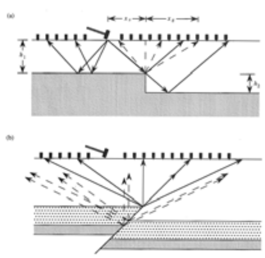

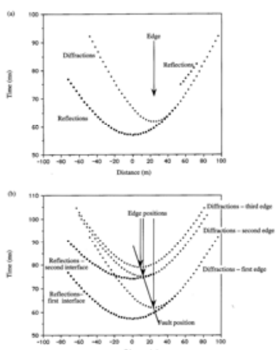

Diffractions and Reflections

Energy over Edge

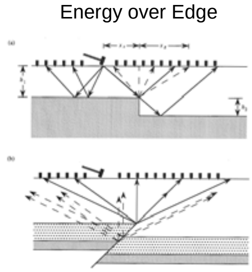

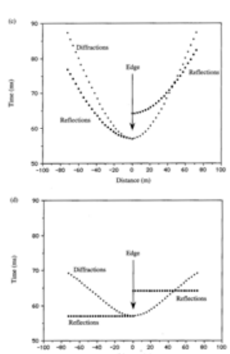

NMO Corrected

Diffraction

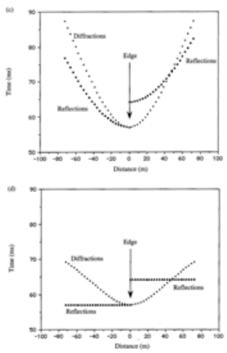

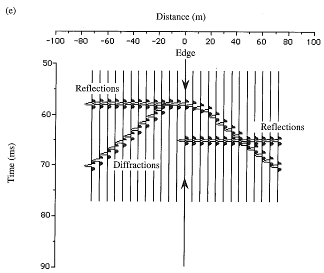

Diffraction

TABLE 4-10 Diffraction Travel-Times

Geophone	Distance (m)	Diffraction Time (ms)	Offset Correction (m)	Total Time (ms)
Source	0	28.6	−9	57.9
1	−3	28.7	−12	57.9
2	−6	28.9	−15	58.2
3	−9	29.3	−18	58.6
4	−12	29.8	−21	59.1
5	−15	30.5	−24	59.8
6	−18	31.3	−27	60.6
7	−21	32.3	−30	61.6
8	−24	33.3	−33	62.6
9	−27	34.5	−36	63.8
10	−30	35.7	−39	65.0
11	−33	37.0	−42	66.3
12	−36	38.4	−45	67.7
13	−39	39.9	−48	69.2
14	−42	41.4	−51	70.7
15	−45	43.0	−54	72.3
16	−48	44.6	−57	73.9
17	−51	46.3	−60	75.6
18	−54	48.0	−63	77.3
19	−57	49.7	−66	79.0
20	−60	51.5	−69	80.8
21	−63	53.3	−72	82.6
22	−66	55.1	−75	84.4
23	−69	57.0	−78	86.3
24	−72	58.8	−81	88.1

Velocity (m/s)	**1400**
Thickness (m)	**40**
Increment 1 (m)	**−3**
Increment 2 (m)	**−3**

Shot offset (m)	**9**
Extra time (ms)	29.3

Vertical & Horizontal Resolution

Fresnel Zone

$$R_1 = \tfrac{1}{2} V_1 \left({t_0}/{f} \right)^{1/2} = \left(\tfrac{1}{2} \lambda h_1 \right)^{1/2} \qquad (4\text{-}61)$$

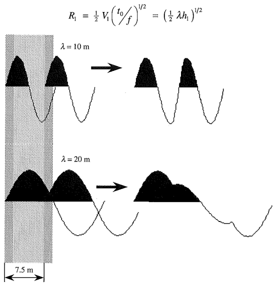

18/3 m versus 42 m Common Offset

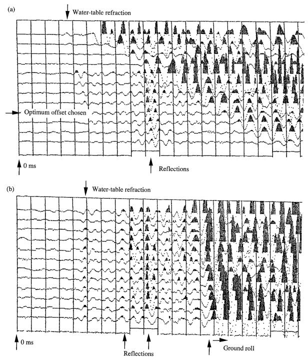

60/3 m versus 60 m Common Offset

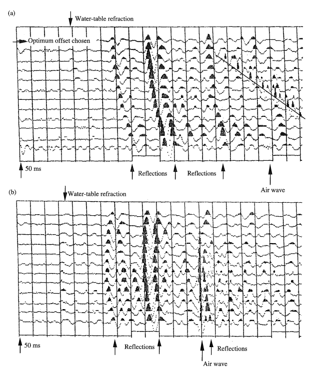

Common Offset (30.5 m) record

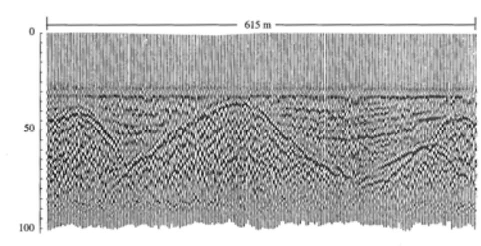

Common Offset: Glacial

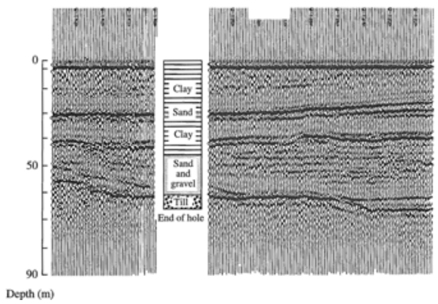

CDP or CMP

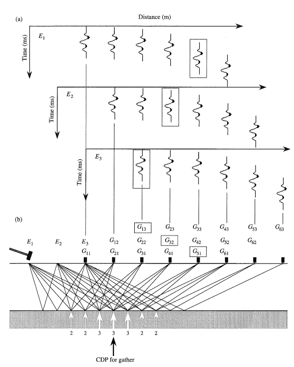

CDP or CMP

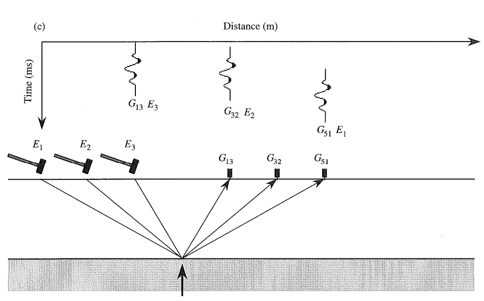

Stacking CDP gathers

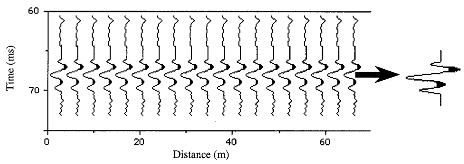

Figure 4-43 CDP gathers corrected for NMO and then stacked to yield waveform of enhanced amplitude.

Static Corrections

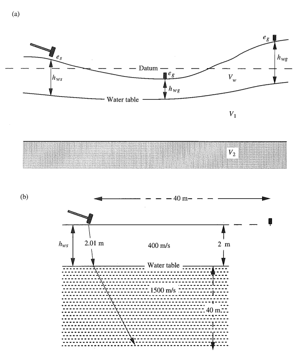

Static Corrections

The first step is to remove the effect of the low-velocity layer. Let t_w represent the weathering correction time. In the case illustrated in Figure 4-39(a) the correction represents the time of travel at 400 m/s less the time of travel at 1500 m/s (essentially we calculate the delay due to this material possessing a velocity of 400 m/s rather than a velocity of 1500 m/s). In mathematical form

$$t_w = \frac{h_w}{V_w} - \frac{h_w}{V_1} \tag{4-62}$$

where h_w represents either h_{wg} or h_{ws}, depending whether we are correcting for the geophone or the shot.

Once the weathering correction is applied, we effectively change the 400-m/s velocity to 1500 m/s. The topographic correction now is applied simply by dividing the difference in elevation between the geophone (or shot) and the datum by, in our example, 1500 m/s. Therefore, the elevation correction is

$$t_e = \frac{e_g - e_d}{V_1} \tag{4-63}$$

Correcting for NMO

Velocity Analysis A. A typical computer program used to facilitate this analysis uses an equation such as Eq. 4-65 to compute the NMO correction.

$$T_{NMO} = \frac{x^2}{2t_0V_{st}^2} - \frac{x^4}{8t_0^3V_{st}^4} \quad (4\text{-}65)$$

Correcting for NMO: Vel. A

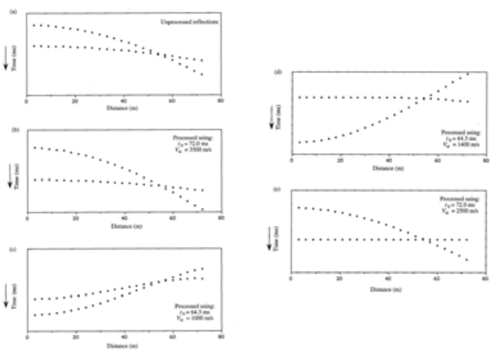

Return to NMO

Recall that the definition of NMO is the difference in reflection travel-times from a horizontal reflecting surface due to variations in the source-geophone distance, or

$$T_{NMO} = t_x - t_0$$

$$T_{NMO} = \frac{\left(x^2 + 4h_1^2\right)^{1/2}}{V_1} - \frac{2h_1}{V_1} \quad (4\text{-}5)$$

Now let's examine our basic travel-time equation once again so that we can express as much as possible in terms of t_0. For convenience in the development we will represent V_1 by V and h_1 by h.

$$t_x = \frac{\left(x^2 + 4h^2\right)^{1/2}}{V} \quad (4\text{-}1)$$

$$t_x^2 = \frac{x^2}{V^2} + \frac{4h^2}{V^2} = \frac{x^2}{V^2} + t_0^2 \quad (4\text{-}40)$$

$$t_x^2 = \frac{x^2 + V^2t_0^2}{V^2} = \left(\frac{x^2}{V^2t_0^2} + 1\right)t_0^2 \quad (4\text{-}41)$$

$$t_x = t_0\left(1 + \frac{x^2}{V^2t_0^2}\right)^{1/2} \quad (4\text{-}42)$$

Return to NMO

According to the generalized binomial theorem,

$$(1 + z)^a = 1 + az + \frac{a(a-1)}{2 \cdot 1} z^2 + \frac{a(a-1)\cdots(a-n+1)}{n!} z^n + \cdots$$

So, if we set

$$a = \frac{1}{2} \quad \text{and} \quad z = \left(\frac{x^2}{V^2 t_0^2}\right)^{1/2}$$

Eq. 4-42 can be expressed as

$$t_x = t_0\left(1 + \frac{x^2}{2V^2 t_0^2} - \frac{x^4}{8V^4 t_0^4} + \frac{x^6}{16V^6 t_0^6} + \cdots\right) \qquad (4\text{-}43)$$

Examining the variables within the parentheses, we see that we can ignore all but the first two terms, *if*

$$\frac{x}{Vt_0} <<< 1$$

If we do so, then our expression reduces to

$$t_x = t_0 + \frac{x^2}{2t_0V^2} \qquad (4\text{-}44)$$

Return to NMO

Recalling our objective to express T_{NMO} in terms of t_0, we see that since

$$T_{NMO} = t_x - t_0$$

then

$$T_{NMO} = \frac{x^2}{2t_0V^2} \qquad (4\text{-}45)$$

However, we must keep in mind the conditions under which Eq. 4-45 is valid. Equation 4-7 tells us that our former qualification

$$\frac{x}{Vt_0} <<< 1$$

is equivalent to saying

$$\frac{x}{2h} <<< 1$$

Thus, for Eq. 4-44 to be a useful approximation, horizontal distance divided by twice the thickness must be much less than one.

$$T_{NMO} = \frac{x^2}{2t_0V^2} - \frac{x^4}{8t_0^3V^4} \qquad (4\text{-}46)$$

$$T_{NMO} = \frac{x^2}{2t_0V_{rms}^2} \qquad (4\text{-}47)$$

NMO Approx: 30-240 m Spread

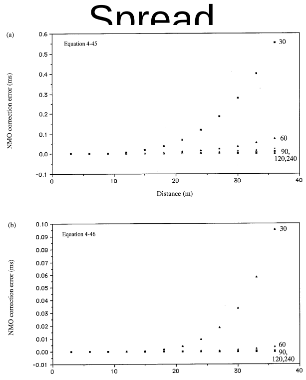

Correcting for NMO

Velocity Analysis C. In this approach we assume that each point on a selected trace is the onset of a possible reflection and then test this assumption on all other traces. Of course, most tests will fail, but some will succeed. In this brief account we concentrate on how such tests are made and how success or failure is determined.

First we utilize Eq. 4-42 and substitute V_{st}.

$$t_x = t_0\left(1 + \frac{x^2}{V_{st}^2 t_0^2}\right)^{1/2} \qquad (4\text{-}66)$$

for the velocity term. If we select a t_0 and a V_{st}, we can calculate reflection times for the source-geophone offsets that we used in our field survey. As we know, these times will plot along a hyperbolic curve. Figure 4-41(a) illustrates a time-distance curve for an actual reflection and two curves determined using Eq. 4-66 and the t_0 and V_{st} values identified in the diagram. Clearly, these are not the correct values, because correct values would produce a curve that plots on the actual reflection curve. Figure 4-41(b) illustrates two curves for which V_{st} is correct but for which t_0 is not.

Correcting for NMO: Vel. C

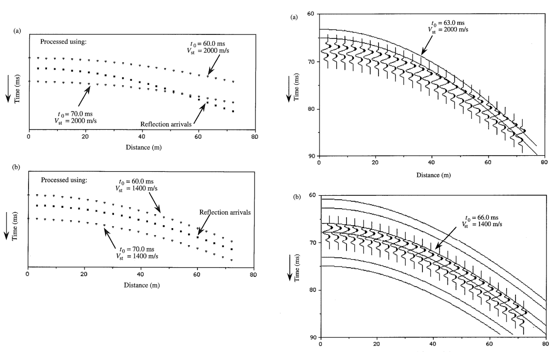

Migration

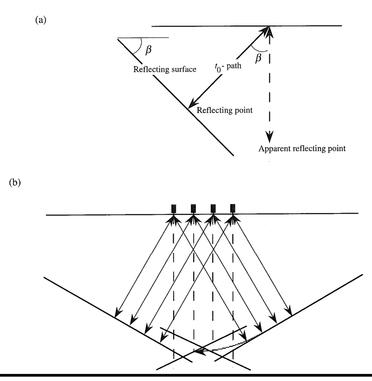

Migration

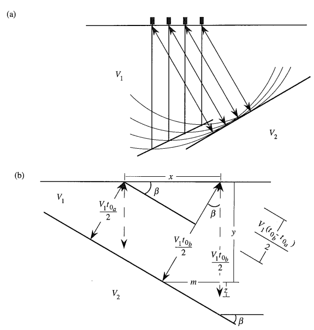

Time Section: Lateral Velocity Variations

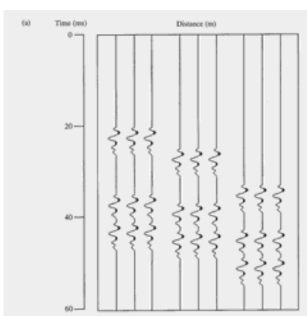

Depth Section

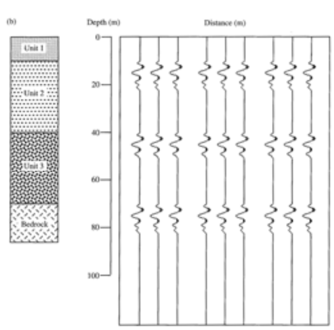

CDP Stack – Meers Fault, OK

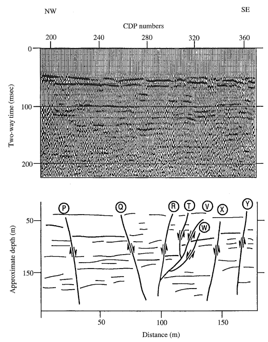

Sinkhole Detection, KS

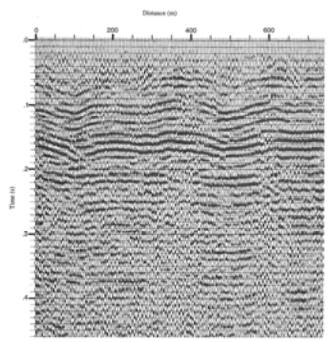

<- Base of Salt

CDP Section: Faults

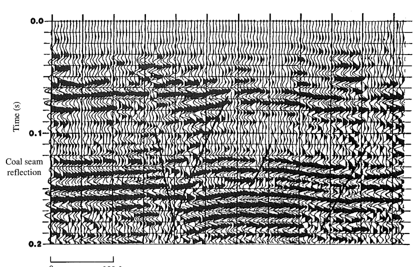

Figure 4-49 CDP seismic section illustrating locations of faults cutting coal seams. (From Gochioco, Lawrence M., and Cotten, Steven A., 1989, Locating faults in underground coal mines using high-resolution seismic reflection techniques: Geophysics, v. 54, p. 1521–1527.)

Split Spread Acquisition

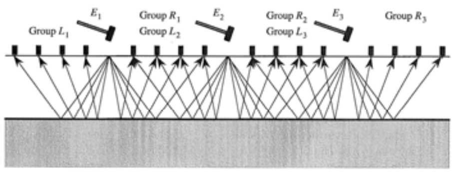

Figure 4-32 A simple form of seismic profiling with single-coverage, center-shot spreads. A 4-geophone spread is shown for simplicity, although shallow-exploration spreads typically contain 12 or 24 geophones.